Unconventional resistivity at the border of metallic antiferromagnetism in NiS_2

P. G. Niklowitz,* P. L. Alireza, M. J. Steiner, and G. G. Lonzarich
Cavendish Laboratory, University of Cambridge, Madingley Road, Cambridge CB3 0HE, United Kingdom

D. Braithwaite, G. Knebel, and J. Flouquet
Département de Recherche Fondamentale sur la Matière Condensée, SPSMS, CEA Grenoble, 38054 Grenoble Cedex 9, France

J. A. Wilson
H. H. Wills Physics Laboratory, University of Bristol, Bristol BS8 1TL, United Kingdom
(Received 26 September 2006; revised manuscript received 18 December 2007; published 27 March 2008)

We report low-temperature and high-pressure measurements of the electrical resistivity $\rho(T)$ of the antiferromagnetic compound NiS_2 in its high-pressure metallic state. The form of $\rho(T,p)$ suggests the presence of a quantum phase transition at a critical pressure $p_c=76\pm5$ kbar. Near p_c, the temperature variation of $\rho(T)$ is similar to that observed in $NiS_{2-x}Se_x$ near the critical composition $x=1$, where metallic antiferromagnetism is suppressed at ambient pressure. In both cases, $\rho(T)$ varies approximately as $T^{1.5}$ over a wide range below 100 K. This lets us assume that the high-pressure metallic phase of stoichiometric NiS_2 also develops itinerant antiferromagnetism, which becomes suppressed at p_c. However, on closer analysis, the resistivity exponent in NiS_2 exhibits an undulating variation with temperature not seen in NiSSe ($x=1$). This difference in behavior may be due to the effects of spin-fluctuation scattering of charge carriers on cold and hot spots of the Fermi surface in the presence of quenched disorder, which is higher in NiSSe than in stoichiometric NiS_2.

DOI: 10.1103/PhysRevB.77.115135 PACS number(s): 71.27.+a, 71.10.−w, 72.80.Ga, 75.40.−s

I. INTRODUCTION

The electronic properties of metals on the border of magnetic phase transitions at low temperatures are often found to exhibit temperature dependences that differ from the predictions of Fermi liquid theory. Early attempts to explore such non-Fermi-liquid behavior have been based on mean-field treatments of the effects of enhanced magnetic fluctuations, as in the self-consistent renormalization (SCR) model.[1–4]

In a recent work, the prediction of this model for the temperature dependence of the electrical resistivity $\rho(T)$ was tested in a simple cubic d metal, Ni_3Al, at high pressures near the critical pressure where ferromagnetism is suppressed.[5] The $T^{5/3}$ temperature dependence of the resistivity seen in Ni_3Al and other related systems, where the magnetic correlation wave vector $\kappa(T)$ is small, appears to be largely consistent with the SCR model.[6] In the idealized limit $\kappa\to0$ at $T\to0$, the SCR model predicts that in three dimensions the quasiparticle scattering rate τ_{qp}^{-1} varies linearly with the quasiparticle excitation energy, rather than quadratically as in the standard Fermi-liquid picture. This form of τ_{qp}^{-1} is similar to that of the marginal Fermi-liquid model,[7–9] which is normally associated with a linear temperature dependence of the resistivity. However, at the border of ferromagnetism, the relevant fluctuations responsible for quasiparticle scattering are of long wavelength and, thus, are ineffective in reducing the current. This leads to a transport relaxation rate τ_{tr}^{-1} that differs from τ_{qp}^{-1} and varies not as T, but as $T^{5/3}$.

In practice, this form of τ_{tr}^{-1} or of the resistivity $\rho(T)$ can be restricted to a relatively narrow range of temperatures and pressures where $\kappa(T)$ is small compared with the characteristic wave vector of thermally excited magnetic fluctuations. The SCR model is not restricted to this limit and can, in principle, include the effects of $\kappa(T)$ and even determine $\kappa(T)$ in a self-consistent fashion. We note that the SCR model assumes implicitly that an effective underlying mechanism exists to remove momentum from the electron system. The validity of this assumption has not been clearly confirmed theoretically, but seems to be consistent with experiment in the cases mentioned above. In its conventional form, the model does not include the possible effects of inhomogeneities or texture that may arise on the border of first order ferromagnetic transitions as in, e.g., MnSi.[13–15] The SCR model is also expected to fail on the border of electron localization as well as near a Mott transition or close to local quantum critical points in heavy electron compounds.[16,17]

The applicability of the SCR model has also been questioned for the case of itinerant-electron antiferromagnetism in general, even well away from the border of a Mott transition.[18–20] In this paper, we present an attempt to test the prediction of the SCR model in a metal assumed to be on the border of metallic antiferromagnetism in three dimensions, for which ρ is predicted to vary as $T^{3/2}$ in the idealized limit $\kappa\to0$, $T\to0$, where κ now stands for the correlation wave vector for the staggered magnetization. The exponent of $3/2$ is the ratio of the spatial dimension $d=3$ and the dynamical exponent $z=2$. This may be contrasted with the corresponding exponent of $5/3$, which is the ratio of $(d+2)=5$ and $z=3$, for the border of metallic ferromagnetism. (The 2 in $d+2$ arises from the effect of small-angle scattering that is absent in the case of the staggered magnetization.) This simple model for the scattering from antiferromagnetic fluctuations assumes that the scattering rate can be averaged over the Fermi surface. Within the SCR model, this procedure would seem to require the presence of a sufficient level of quenched disorder assumed to have only the simple consequence of inhibiting the short circuiting caused by the carrier on the cold spots of the Fermi surface, i.e., regions far from the hot spots connected by the antiferromagnetic ordering

wave vector and, thus, strongly affected by spin-fluctuation scattering.[18–20]

The effect of quenched disorder on the temperature dependence of ρ in the SCR model shows up particularly clearly in the temperature-dependent resistivity exponent defined as $n=\partial \ln \Delta\rho / \partial \ln T$, where $\Delta\rho=\rho(T)-\rho_0$ and ρ_0 is the residual resistivity, i.e., the resistivity extrapolated to $T=0$ K. The resistivity exponent n may be described in terms of the Fermi wave vector k_F, the elastic mean free path l of charge carriers, and the reduced temperature $t=T/T_{sf}$, where T_{sf} is a characteristic spin fluctuation temperature.[6] With increasing t, n drops from 3/2 toward unity around $t \approx 1/k_F l$, back toward a value of the order of 3/2 around $t \approx 1/\sqrt{k_F l}$, and then toward zero for $t \gg 1/k_F l$.[18–20] This undulating behavior of n is a dramatic prediction of the model for relatively pure samples that could, in principle, be tested by studying a series of samples of the same material with different levels of quenched disorder. Rosch[19,20] introduced this model in an effort to understand the temperature dependence of the resistivity exponent measured for the f-electron metal $CePd_2Si_2$.[21,22] The results were, in this case, not entirely conclusive because of the anisotropic and complex nature of the spin fluctuation spectrum in this material.

Here, we present a test of Rosch's model in a d-electron system with a cubic structure and T_{sf} 1–2 orders of magnitude greater than in typical heavy f-electron systems. We compare the temperature dependence of ρ of two closely related systems on the border of antiferromagnetism. The two materials are NiS_2 near 76 kbar and $NiS_{2-x}Se_x$ for $x=1$, where the Néel temperature T_N vanishes at ambient pressure. Due to random variations in the locations of the S and Se atoms in the lattice, values of ρ_0 found in NiSSe are typically 1 order of magnitude higher than in stoichiometric NiS_2 compounds.

NiS_2 crystallizes in the cubic pyrite structure and is an antiferromagnetic insulator at ambient pressure at low temperatures.[23,24] It can be metallized via the application of pressure[25–28] (approximately 25–30 kbar) or by Se substitution.[10,12,25–27,29,30] The temperature-pressure phase diagram of NiS_2 and the temperature-composition phase diagram of $NiS_{2-x}Se_x$ (Fig. 1) are expected to be similar, as suggested by the correspondence of the temperature-pressure and temperature-composition phase diagrams of NiS_2 found in earlier work.[10,12,29,30] Of particular interest for this paper is the boundary of metallic antiferromagnetism that appears (i) at $x \cong 1$, i.e., for NiSSe, in temperature-composition phase diagram (Fig. 1), (ii) is assumed to appear at p_c in the temperature-pressure phase diagram for stoichiometric NiS_2. We note that in both cases, the quantum phase transition from metallic antiferromagnetism to paramagnetism would arise well beyond the metal-insulator transition (see Fig. 1 for the case where composition is the control parameter).

We present a high-pressure study of the temperature dependence of the resistivity of NiS_2 in the metallic state, which reveals a critical pressure $p_c \cong 76$ kbar. The results at p_c are compared with that of NiSSe at ambient pressure reported in Ref. 12. In both materials, one observes a non-Fermi-liquid form of the resistivity that appears in first approximation to be consistent with the predictions of the SCR model (inset of Fig. 1 for NiSSe). However, the resistivity of

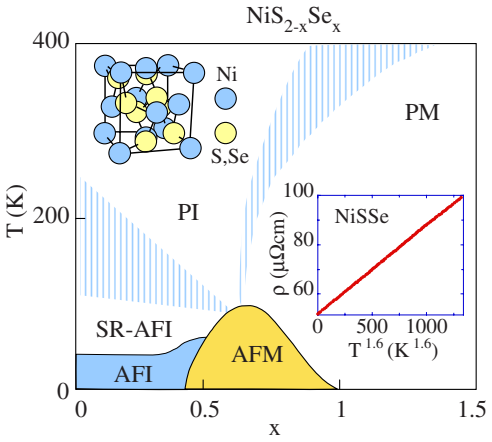

FIG. 1. (Color online) Temperature-composition phase diagram of $NiS_{2-x}Se_x$ (Refs. 10 and 11). Lower inset shows the temperature dependence of the resistivity of NiSSe ($x=1$), which is just on the border of a metallic antiferromagnetic state at low temperatures (Ref. 12). The upper inset is the pyrite crystal structure of NiS_2 and $NiSe_2$. PI and PM stand for paramagnetic insulator and paramagnetic metal, respectively. AFI and AFM stand for antiferromagnetic insulator and antiferromagnetic metal, respectively. SR-AFI stands for short range antiferromagnetic insulator (Ref. 11). The temperature-pressure phase diagram of NiS_2 is expected to be similar in form to the temperature-composition phase diagram of $NiS_{2-x}Se_x$. In this study, the AFM boundary of NiS_2 is found to be at $p_c=76\pm5$ kbar. Thus, NiS_2 at p_c and NiSSe at ambient pressure may be expected to be similar except for the level of quenched disorder, which is normally higher in NiSSe than in NiS_2. The residual resistivity of NiSSe is typically an order of magnitude higher than in NiS_2.

NiS_2 near p_c has an undulating component in its variation with temperature that is not seen in NiSSe. This difference in behavior might arise from the effects of cold and hot spots on the Fermi surface as suggested by the model due to Rosch discussed above.[19,20]

II. EXPERIMENT

Single crystals of NiS_2 have been grown by chemical vapor transport using iodine as the transport agent.[25] The residual resistivity ratio $[\rho(273\ \text{K})/\rho_0]$ above 50 kbar is about 30 for our samples, compared with about 3 for NiSSe.[12] The carrier mean free path of NiS_2 is, thus, expected to be about an order of magnitude higher than in NiSSe.

Pressure was applied by means of a nonmagnetic Bridgman cell using tungsten carbide anvils. The cell used is a scaled down version of that designed by Wittig.[31] The cullet diameter of the anvils was 3.5 mm. The gasket was made of pyrophyllite with a central hole to accommodate the NiS_2 sample as well as a Pb sample and the steatite pressure-transmission medium. After compression, the sample space was reduced to about 1.5 mm in diameter and 0.1 mm in thickness. The pressure was determined from the superconducting transition temperature of the Pb sample.[32] The width of the superconducting transition suggested that the pressure variation over the Pb sample was about 10% of the average pressure.

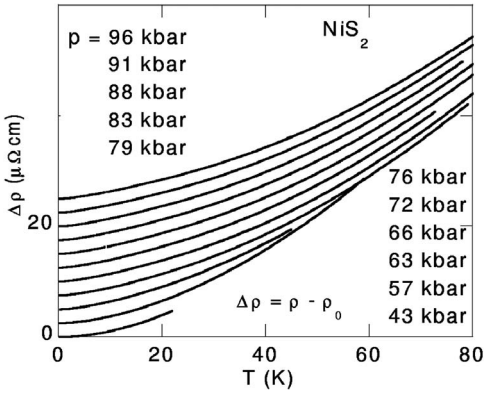

FIG. 2. Temperature dependence of the resistivity in the metallic state of NiS_2 at high pressures. $\Delta\rho$ is $\rho(T)-\rho_0$, where ρ_0 is the residual resistivity extrapolated to $T=0$ K. The curves are shifted vertically for clarity.

The resistivity was measured via the four-terminal ac technique. Four 50 μm Pt leads were passed into the high-pressure region via grooves in the insulating pyrophyllite gasket. The bare wires were rested on top of the samples and pressed onto the sample surface during pressurization to achieve adequate electrical contacts.

The resistivity measurements were carried out with two different and independent systems, a helium circulation cryostat (ILL Orange cryostat; 1.5–300 K) in Grenoble and an adiabatic demagnetization refrigerator (0.04–100 K) in Cambridge. The latter system had two voltage channels, one with a low-temperature transformer and the other with a room-temperature transformer. The excitation currents were 1 mA and 160 μA in the Orange cryostat and in the adiabatic demagnetization fridge, respectively. The results obtained with these two experimental systems were consistent with each other where comparisons could be made.

III. RESULTS

The temperature variations of the resistivity of NiS_2 in the high-pressure metallic state above 40 kbar are presented in Fig. 2 and 3. [The insulator-to-metal transition (not shown) was observed at around 30 kbar, in agreement with the literature.[25]] Figure 2 shows $\Delta\rho$ vs T up to 80 K, and Fig. 3 is an expanded view of $\Delta\rho$ vs T in the range 0.05–2 K.

Below 1 K, the resistivity can be described by an equation of the form $\rho=\rho_0+AT^2$ over the entire pressure range explored, 43–96 kbar. The pressure variations of the fitted values of A and ρ_0 are given in Fig. 4. The T^2 coefficient A exhibits a peak at $p_c=76\pm5$ kbar.

Figures 5 and 6 compare $\Delta\rho$ vs T^2 and $\Delta\rho$ vs $T^{3/2}$, respectively, in three panels each covering different ranges in temperature. Figure 5(c), in particular, highlights the T^2 variation observed at all pressures with a peak of A at around p_c as discussed above. Figures 6(a)–6(c) and 7, on the other hand, suggest that near this pressure $\Delta\rho$ varies roughly as $T^{3/2}$ over a decade in temperature above a few Kelvin. This is the behavior predicted by the SCR model for a system on the border of metallic antiferromagnetism as discussed in the

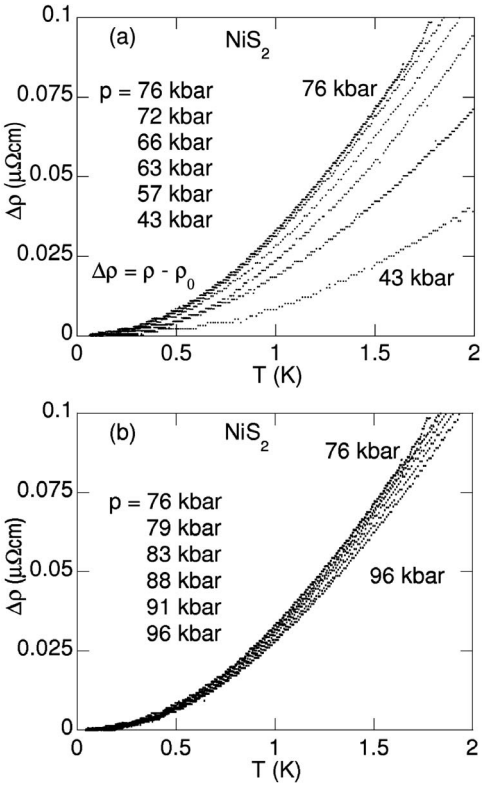

FIG. 3. Low temperature variation of the resistivity in the metallic state of NiS_2 at high pressures. $\Delta\rho$ grows in strength up to 76 kbar (a) and weakens gradually above 76 kbar (b).

Introduction. The existence of a T^2 regime even at p_c, however, suggests that the transition into the antiferromagnetic state below p_c may not be continuous, i.e., that the antiferromagnetic quantum critical point is not quite reached due to the onset of a first order transition (see discussion). We note that the weak pressure variation of the Fermi-liquid (FL) crossover temperature T_{FL} near p_c (see Fig. 7 and the caption) would seem to rule out an explanation of the T^2 resistivity in terms of an inhomogeneity in pressure.

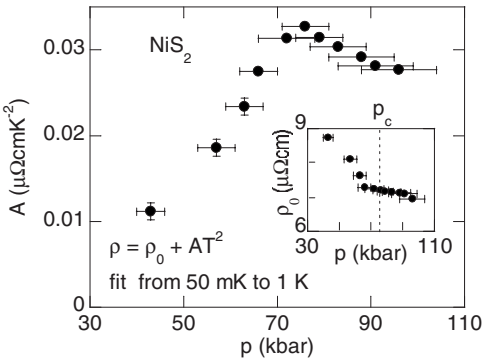

FIG. 4. The T^2 coefficient of the resistivity, A, and residual resistivity, ρ_0 (inset), of NiS_2 in the metallic high-pressure state. The parameters A and ρ_0 are obtained by a fit of the resistivity as indicated in the figure (where no error bar is plotted, the error is smaller than the point thickness). A is peaked at $p_c=76\pm5$ kbar. This marks the boundary of the metallic antiferromagnetic state of NiS_2.

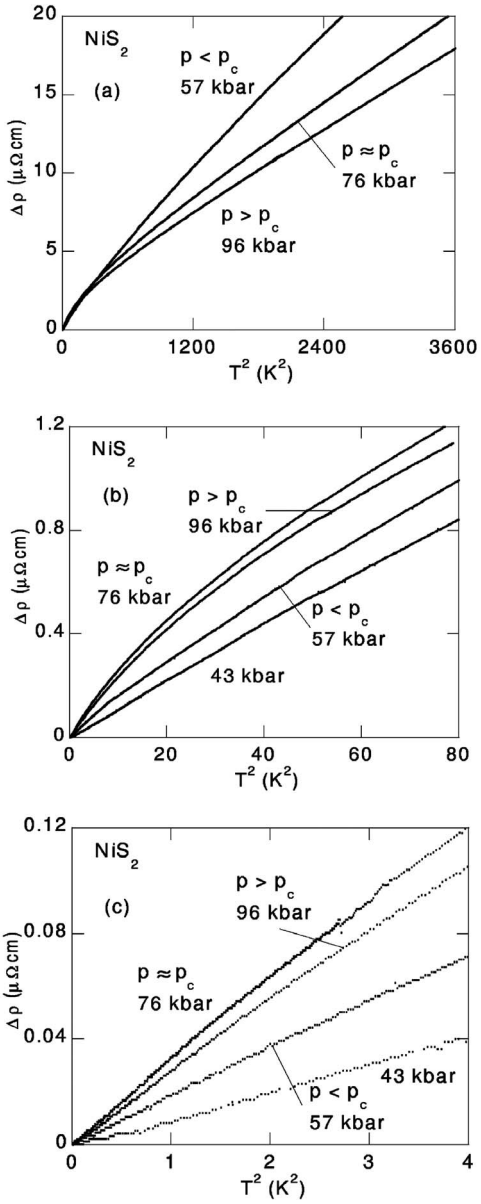

FIG. 5. Resistivity vs T^2 in the high-pressure metallic regime of NiS_2. The three panels are for different temperature intervals. A quadratic temperature dependence of $\Delta\rho$ is seen only at the lowest temperatures (below a few Kelvin) and the T^2 coefficient of $\Delta\rho$ is peaked at $p_c \approx 76$ kbar as shown in Fig. 4.

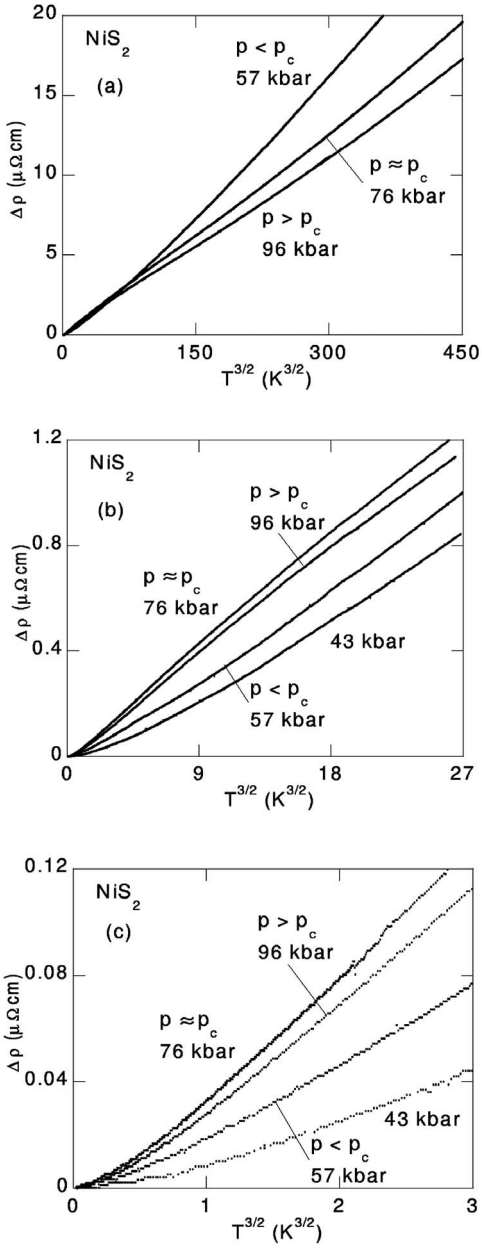

FIG. 6. Resistivity vs $T^{3/2}$ in the high-pressure metallic regime of NiS_2. The three panels are for different temperature intervals. An approximately $T^{3/2}$ variation of $\Delta\rho$ is seen around $p_c \approx 76$ kbar only over a decade in temperature above a few Kelvin. $\Delta\rho$ is quadratic in temperature below a few Kelvin at all pressures in the metallic regime studied [see Fig. 5(c)].

The identification of p_c with the boundary of metallic antiferromagnetism is also suggested by the correspondence of the temperature-pressure phase diagram of NiS_2 and the temperature-composition phase diagram of $NiS_{2-x}Se_x$ found in earlier work.[10,12,29,30] This predicted that the critical pressure for the border of metallic antiferromagnetism should be around 60 kbar, which is of the same order of magnitude as p_c defined above. The identification of p_c with the antiferromagnetic boundary in the metallic state is tentative and needs confirmation by other measurements and, in particular, the detection of a signature of T_N in the resistivity for pressures below p_c. Here, we focus attention mainly on the behavior of ρ near p_c and contrast it with that of NiSSe at ambient pressure (inset of Fig. 1).

The non-Fermi-liquid behavior of $\Delta\rho$ over a wide temperature range near p_c (low-temperature data at 76 kbar combined with 77 kbar data up to 300 K; the high-temperature data is scaled to match the low-temperature data; the data sets overlap between 5 and 70 K) is highlighted in Fig. 8. Figure 8(a) shows the dramatic upturn of $\Delta\rho/T^2$, which in the Fermi-liquid regime is expected to saturate to a constant value. Figure 8(b) is a plot of $\ln \Delta\rho$ vs $\ln T$, which shows that the average slope corresponds to a resistivity exponent close to 3/2, as discussed above and as seen in NiSSe at ambient pressure. However, in contrast to NiSSe, the temperature de-

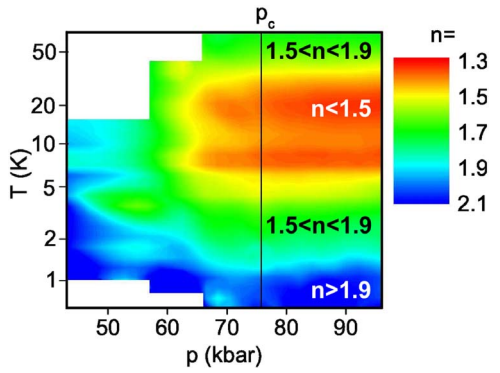

FIG. 7. (Color online) The resistivity exponent $n = \partial \ln \Delta\rho / \partial \ln T$ in the temperature-pressure plane for NiS_2 in the metallic regime. A Fermi-liquid temperature dependence of the resistivity with $n \approx 2$ is seen at the lowest temperatures. The Fermi-liquid range seems to have a minimal extension with $T_{FL} < 2$K close to $p_c \approx 76$ kbar, although the pressure dependence above p_c is weak. A non-Fermi-liquid T^n form of the resistivity with $n \approx 3/2$ is seen over approximately a decade in temperature above a few Kelvin near p_c.

pendence of the resistivity in NiS_2 at p_c exhibits an undulating structure which is evident in Fig. 8(b) and highlighted in the temperature dependence of the resistivity exponent $n = \partial \ln \Delta\rho / \partial \ln T$ shown in the inset. We note that this undulating structure has been observed in several samples of NiS_2 and in two independent measurement systems.

IV. DISCUSSION

The resistivity measurements suggest that antiferromagnetism in the high-pressure metallic state of NiS_2 is suppressed at a critical pressure of $p_c = 76 \pm 5$ kbar. At p_c, we find that the T^2 coefficient of the low-temperature resistivity A has its maximum and the Fermi-liquid crossover temperature T_{FL} defined in the caption of Fig. 7 seems to be at a minimum close to p_c, although the pressure dependence is weak above p_c. Above T_{FL}, near p_c the resistivity has an approximately $T^{3/2}$ temperature dependence over a decade in temperature. As already stated, this is the behavior expected in the SCR model for a metal in three dimensions on the border of antiferromagnetism at low temperatures. Also, we note that p_c is of the same order of magnitude as that inferred for the correspondence between the temperature-composition and temperature-pressure phase diagrams as discussed in the previous section.

This suggests that magnons cause non-Fermi-liquid behavior in NiS_2. Non-Fermi-liquid behavior due to magnons follows, in the SCR model, from an underlying quasiparticle scattering rate that varies linearly with the excitation energy E of a quasiparticle near the Fermi level (the scattering rate is proportional to E^2 for quasiparticles in a Fermi liquid).[1–4] It is improbable that T_{FL} merely marks the onset of phonon scattering, as its contribution should be negligible at low temperatures. There is no other likely scattering mechanism which could mask Fermi-liquid behavior at low temperatures.

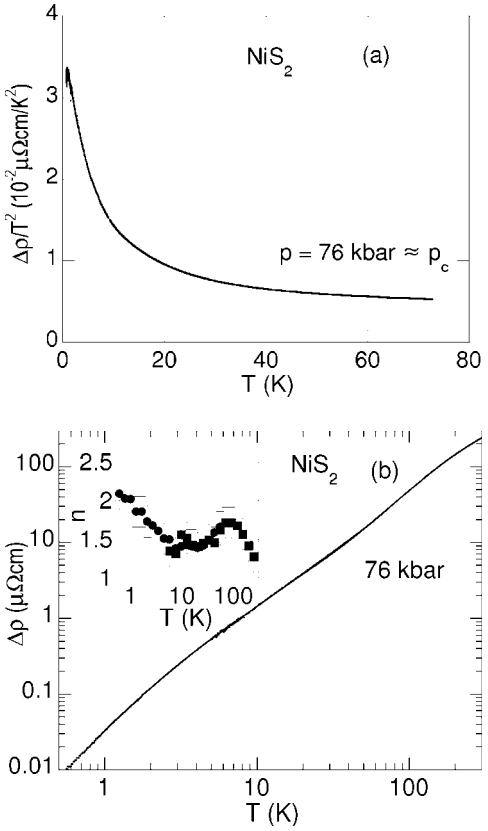

FIG. 8. The non-Fermi-liquid form of the resistivity of NiS_2 near $p_c \approx 76$ kbar. (a) $\Delta\rho/T^2$ vs T does not saturate and, thus, has a non-Fermi-liquid form over a wide temperature range, except at very low temperatures (Fig. 5(b)). A plot of $\ln \Delta\rho$ vs $\ln T$ and the resistivity exponent $n = \partial \ln \Delta\rho / \partial \ln T$ vs $\ln T$ (inset: circles and squares determined from low- and high-temperature data sets, respectively) exhibits an undulating form in contrast to the simple $T^{1.6}$ temperature dependence seen in NiSSe (Ref. 12 and Fig. 1). This undulating form of the resistivity has been seen in different NiS_2 specimens and with two independent measurement systems.

The weakness or absence of a signature of T_N in the resistivity below p_c is not necessarily surprising since the same is the case for $NiS_{2-x}Se_x$ in the range $0.4 \leqslant x \leqslant 1$,[12,33] where antiferromagnetic order has been confirmed by neutron scattering.[10,34,35] The signature of T_N in ρ can be washed out by inhomogeneities in composition or pressure and may only show up in high-precision measurements of $\partial\rho/\partial T$ in the pressure range where T_N is not too strongly varying with pressure and where pressure is hydrostatic.

The fact that T_{FL} and, correspondingly, the T^2 coefficient of the low-temperature resistivity A remain finite at p_c is not necessarily inconsistent with our assumption that p_c marks the border of antiferromagnetism. The antiferromagnetic transition vs pressure may be first order as is found in a number of antiferromagnetic metals such as YMn_2 and $GdMn_2$.[36] However, the observation of a clear increase of A toward p_c suggests that the transition is only weakly first order, i.e., κ stays finite but is reduced to a small value toward p_c. Low-energy spin fluctuations are frozen out in an energy interval proportional to κ^2, which explains the pressure dependence of T_{FL} and the observation of a T^2 resistiv-

ity in a small low-temperature interval even at p_c. We note that first order quantum phase transitions also seem to be common in ferromagnetic metals such as MnSi and Ni_3Al.[5,37,38] T_{FL} and A remain finite at the antiferromagnetic boundary of YMn_2, a system that shares some features in common with NiS_2. (We note, however, that the absence of Fermi-liquid behavior does not necessarily mean that the quantum phase transition is continuous.[13,14])

The Fermi-liquid crossover temperature T_{FL} in NiS_2 is very much lower than the characteristic spin fluctuation temperature T_{sf} which may be expected to be of the order of 10^3 K in a typical d metal. We consider to what extent the behavior above T_{FL}, but below T_{sf}, may be understood in terms of an itinerant-electron model for a continuous antiferromagnetic quantum critical point. The predictions of the SCR model as analyzed by Rosch have already been outlined in the Introduction for an antiferromagnetic quantum critical point. With increasing reduced temperature $t=T/T_{sf}$, the SCR model predicts that the resistivity exponent $n=\partial \ln \Delta\rho/\partial \ln T$ drops from an initial value of 3/2 toward unity around $t \approx 1/k_F l$, back to a value of order 3/2 around $t \approx 1/\sqrt{k_F l}$, and then to zero for $t \gg 1/k_F l$.[18–20] This behavior is qualitatively similar to that seen in NiS_2 at p_c and above T_{FL} (inset of Fig. 8). For reasonable choices of parameters for NiS_2, $T_{sf} \approx 10^3$ K, $k_F \approx 0.5$ Å^{-1}, and $l \approx 140$ Å^{-1},[39] we expect the minimum of n to occur near 15 K and the maximum at around 120 K. These crossover temperatures are in rough agreement with our observations.

In NiSSe, l is an order of magnitude smaller than in NiS_2 and, thus, the minimum and maximum of n are expected to arise at around 100 and 320 K, respectively. Over the temperature range of the experiments shown in the inset of Fig. 1, the model predicts a simple $T^{3/2}$ temperature dependence without modulation, as is seen. The difference in the behavior of NiS_2 and NiSSe at their respective critical conditions is, thus, not surprising. The combined effects of scattering from spin and lattice fluctuations might also lead to an undulating behavior of n, but this would naively be expected to arise in both NiS_2 and NiSSe, in contradiction with observation. A systematic study of NiS_2 samples with different purity levels and inclusion of multiband effects in the analysis will be necessary to further clarify the origin of the observed undulating behavior of the resistivity exponent.

V. CONCLUSIONS

Enhanced scattering in the electrical resistivity of NiS_2 around $p_c = 76 \pm 5$ kbar is believed to indicate a quantum phase transition from an assumed metallic antiferromagnetic to a paramagnetic state. The temperature dependence of the resistivity near p_c is consistent with that expected for a metal on the border of itinerant-electron antiferromagnetism. The Fermi-liquid crossover temperature T_{FL}, which defines the range over which the resistivity is roughly quadratic in temperature, does not vanish at p_c, but is 3 orders of magnitude smaller than the characteristic spin fluctuation temperature T_{sf}. The finite value of T_{FL} may indicate that the antiferromagnetic quantum critical point is first order, as is the case in related materials such as YMn_2.

Over a wide temperature range above T_{FL}, the temperature variation of the resistivity exhibits a non-Fermi-liquid form that can be understood in terms of the effects of spin-fluctuation scattering at cold and hot spots of the Fermi surface as anticipated by Rosch in his refined treatment of the SCR model. In particular, the resistivity exponent $n=\partial \ln \Delta\rho/\partial \ln T$ exhibits an undulating structure which is consistent not only qualitatively, but also approximately quantitatively with the predictions of this model. The model also accounts for the absence of this undulating structure in the related, but less pure material, NiSSe, which is known to be at the border of antiferromagnetism at ambient pressure.

Note added. Recently, another paper[40] on transport properties of NiS_2 under pressure appeared, displaying results which are broadly in agreement with our measurements.

ACKNOWLEDGMENTS

We thank A. Rosch and S. Julian for valuable discussions. P.G.N. is grateful for support from the FERLIN program of the European Science Foundation.

*Present address: Department of Physics, Royal Holloway, University of London, Egham TW20 0EX, UK; philipp.niklowitz@rhul.ac.uk

[1] J. A. Hertz, Phys. Rev. B **14**, 1165 (1976), and references therein.
[2] A. J. Millis, Phys. Rev. B **48**, 7183 (1993), and references therein.
[3] T. Moriya, *Spin Fluctuations in Itinerant Electron Magnetism* (Springer, Berlin, 1985), and references therein.
[4] G. G. Lonzarich, in *Electron*, edited by M. Springford (Cambridge University Press, Cambridge, England, 1997), Chap. 6, pp. 109–147.
[5] P. G. Niklowitz, F. Beckers, G. G. Lonzarich, G. Knebel, B. Salce, J. Thomasson, N. Bernhoeft, D. Braithwaite, and J. Flouquet, Phys. Rev. B **72**, 024424 (2005).
[6] J. Mathon, Proc. R. Soc. London, Ser. A **306**, 355 (1968).
[7] C. M. Varma, P. B. Littlewood, S. Schmitt-Rink, E. Abrahams, and A. E. Ruckenstein, Phys. Rev. Lett. **63**, 1996 (1989).
[8] T. Holstein, R. E. Norton, and P. Pincus, Phys. Rev. B **8**, 2649 (1973).
[9] G. Baym and C. Pethick, *Landau-Fermi Liquid Theory* (Wiley, New York, 1991), Chap. 3.
[10] M. Matsuura, H. Hiraka, K. Yamada, and Y. Endoh, J. Phys. Soc. Jpn. **69**, 1503 (2000).
[11] J. M. Honig and J. Spałek, Chem. Mater. **10**, 2910 (1998).
[12] S. Miyasaka, H. Takagi, Y. Sekine, H. Takahashi, N. Mori, and R. J. Cava, J. Phys. Soc. Jpn. **69**, 3166 (2000).
[13] C. Pfleiderer, S. R. Julian, and G. G. Lonzarich, Nature (London) **414**, 427 (2001).
[14] N. Doiron-Leyraud, I. R. Walker, L. Taillefer, M. J. Steiner, S. R.

Julian, and G. G. Lonzarich, Nature (London) **425**, 595 (2003).
[15] D. Belitz, T. R. Kirkpatrick, and T. Vojta, Phys. Rev. Lett. **82**, 4707 (1999).
[16] P. Coleman, C. Pépin, Q. Si, and R. Ramazashvili, J. Phys.: Condens. Matter **13**, R723 (2001).
[17] Q. Si, S. Rabello, K. Ingersent, and J. L. Smith, Nature (London) **413**, 804 (2001).
[18] R. Hlubina and T. M. Rice, Phys. Rev. B **51**, 9253 (1995).
[19] A. Rosch, Phys. Rev. Lett. **82**, 4280 (1999).
[20] A. Rosch, Phys. Rev. B **62**, 4945 (2000).
[21] S. R. Julian *et al.*, J. Magn. Magn. Mater. **177-181**, 265 (1998).
[22] F. M. Grosche, M. J. Steiner, P. Agarwal, I. R. Walker, D. M. Freye, S. R. Julian, and G. G. Lonzarich, Physica B **281**, 3 (2000).
[23] D. W. Bullett, J. Phys. C **15**, 6163 (1982).
[24] A. Y. Matsuura, H. Watanabe, C. Kim, S. Doniach, Z.-X. Shen, T. Thio, and J. W. Bennett, Phys. Rev. B **58**, 3690 (1998).
[25] J. A. Wilson and G. D. Pitt, Philos. Mag. **23**, 1297 (1971).
[26] J. A. Wilson, Adv. Phys. **21**, 143 (1972).
[27] J. A. Wilson, in *The Metallic and Non-Metallic States of Matter*, edited by P. P. Edwards and C. N. R. Rao (Taylor & Francis, London, 1985), Chap. 9, pp. 215–260.
[28] Y. Sekine, H. Takahashi, N. Mori, T. Matsumoto, and T. Kosaka, Physica B **237-238**, 148 (1997).
[29] N. Mori and H. Takahashi, J. Magn. Magn. Mater. **31-34**, 335 (1983).
[30] A. Husmann, J. Brooke, T. F. Rosenbaum, X. Yao, and J. M. Honig, Phys. Rev. Lett. **84**, 2465 (2000).
[31] J. Wittig, Z. Phys. **195**, 215 (1966).
[32] A. Eichler and J. Wittig, Z. Angew. Phys. **25**, 319 (1968).
[33] X. Yao, J. M. Honig, T. Hogan, C. Kannewurf, and J. Spalek, Phys. Rev. B **54**, 17469 (1996).
[34] S. Sudo and T. Miyadai, J. Phys. Soc. Jpn. **54**, 3934 (1985).
[35] S. Sudo, J. Magn. Magn. Mater. **114**, 57 (1992).
[36] R. Hauser, A. Indinger, E. Bauer, and E. Gratz, J. Magn. Magn. Mater. **140-144**, 799 (1995).
[37] C. Pfleiderer, G. J. McMullan, S. R. Julian, and G. G. Lonzarich, Phys. Rev. B **55**, 8330 (1997).
[38] C. Thessieu, C. Pfleiderer, A. N. Stepanov, and J. Flouquet, J. Phys.: Condens. Matter **9**, 6677 (1997).
[39] The order of magnitude, T_{sf}, was estimated from the value of A in the SCR model, k_F from the size of the Brillouin zone and electron filling of the bands, and l from ρ_0.
[40] N. Takeshita, S. Takashima, C. Terakura, H. Nishikubo, S. Miyasaka, M. Nohara, Y. Tokura, and H. Takagi, arXiv:0704.0591 (unpublished).